# The Role of Thymoquinone in Mitigating Carbon Tetrachloride-Induced Hepatocellular Carcinoma in Rats: Targeting the CHOP-1/JNK/P38 MAPK, NFκB/TNF-α/IL-10, and Bax/Bcl-2/Caspase-3 Signalling Pathways

Rania Elsayed HUSSEIN, Laila Ahmed RASHED, Basma Emad ABOULHODA iD,
Ghada Mahmoud ABDELAZIZ, Ebtehal Gamal ABDELHADY, Sarah A. Abd EL-AAL,
Asmaa SHAMSELDEEN, Mohamed Mansour KHALIFA, and Heba MORSI

Original article

The present study was conducted to evaluate the effect of thymoquinone (TQ) on hepatocellular carcinoma (HCC) in rats. Our study has reported that TQ treatment of experimentally-induced HCC results in the up-regulation of the Jun-N-terminal kinase and p38 mitogen activated protein kinase pathway (JNK/p38 MAPK) and the enhancement of anti-inflammatory, anti-oxidant, and pro-apoptotic machineries. TQ resulted in a significant decrease in the levels of nuclear factor kappa-light-chain-enhancer of activated B-cells (NFκB), tumor necrosis factor-α (TNF-α), and a significant increase in the anti-inflammatory interleukin-10 (IL-10). The pro-apoptotic effect of TQ was demonstrated through stimulating the apoptotic Bcl-2-associated X (Bax) gene and inhibiting the anti-apoptotic B-cell lymphoma 2 (Bcl-2) gene together with increasing the level of caspase 3 and up-regulating the C/EBP homologous protein (CHOP-1) gene expression. TQ treatment also enhanced the activity of the ROS scavenger, superoxide dismutase (SOD), and decreased the level of the lipid peroxidation product malondialdehyde (MDA). TQ-dependent suppression of HCC was associated with the up-regulation of JNK/p38 MAPK, enhanced CHOP-1 expression, and subsequently increased Bax gene expression.

Key words: HCC, thymoquinone, JNK, p38-MAPK, apoptosis.

*Rania Elsayed HUSSEIN, Laila Ahmed RASHED, Heba MORSI, Department of Medical Biochemistry and Molecular Biology, Faculty of Medicine, Cairo University, Egypt.*
*Basma Emad ABOULHODA, Department of Anatomy and Embryology, Faculty of Medicine, Cairo University, Egypt.*
*E-mail: basma.emad@kasralainy.edu.eg*
*Ghada Mahmoud ABDELAZIZ, Ebtehal Gamal ABDELHADY, Department of Medical Biochemistry and Molecular Biology, Faculty of Medicine, Beni-Suef University, Egypt.*
*Sarah A. Abd EL-AAL, Pharmacology and Toxicology Division, Department of pharmacy, Kut University College, Al Kut, Wasit, Iraq, 52001.*
*Asmaa SHAMSELDEEN, Mohamed Mansour KHALIFA, Department of Physiology, Faculty of Medicine, Cairo University, Egypt.*
*Mohamed Mansour KHALIFA, Department of Physiology, Faculty of Medicine, King Saud University, KSA.*

Hepatocellular carcinoma (HCC) accounts for 85-90% of all primary liver cancers and is the third leading cause of cancer-related deaths worldwide (OZAKYOL 2017). Endoplasmic reticulum (ER) stress can lead to ER dysfunction in the terminal phase (BHAT *et al.* 2013), thus triggering an unfolded protein response (UPR). The UPR has a dual function in cells. One function is to alleviate damage and promote homeostasis in cells, and the other is to induce a pro-apoptotic effect in cells exposed to chronic or overwhelming ER stress (WANG *et al.* 2014).

The key regulator of ER stress-induced apoptosis is the C/EBP homologous protein (CHOP). Generally, the role of autophagy in liver cancer is dynamic and changeable (CHANG *et al.* 2012). CHOP can also regulate the Bax and Bcl-2 family. Thus, overexpression of CHOP can induce cell cycle arrest leading to cell apoptosis; even more CHOP-deficient cells were

resistant to ER stress-induced apoptosis (HU *et al.* 2019).

Both c-Jun NH$_2$-terminal kinase (JNK) and the p38 mitogen activated protein kinase family (p38 MAPK) are the upstream regulators of CHOP. They cooperate together to regulate apoptosis (PARK *et al.* 2014). P38 dis-regulation is implicated in the development of solid tumors, such as lung and liver cancers (IYODA *et al.* 2003). Both *in-vivo* and *in-vitro* studies have demonstrated that the initiation of HCC was inhibited upon activation of the reactive oxygen species/p38 MAPK pathway (CHIBA *et al.* 2014).

The potential anti-neoplastic role of thymoquinone (TQ) is mediated via inhibition of cell proliferation, the activation of cell cycle arrest, and the triggering of anti-inflammatory, pro-apoptotic, and anti-oxidant mechanisms (HARON *et al.* 2018). The contribution of oxidative stress in promoting hepatocarcingenesis was confirmed. In the ovarian cancer cell line, the anti-cancer effect of TQ involves the activation of apoptosis and cellular oxidative stress. In renal carcinoma, Caki cell lines incubated with TQ (75 $\mu$M), the key anti-apoptotic factor, Bcl-2, was suppressed in a dose dependent manner causing apoptosis (PARK *et al.* 2016).

Thus, the present study was designed to evaluate the efficacy of using thymoquinone in experimentally-induced HCC and to assess the hepatocellular signalling of JNK/p38 MAPK and the downstream CHOP-regulated pathways.

## Materials and Methods

This study was performed at the Unit of Molecular Biology at the Medical Biochemistry and Molecular Biology, Physiology, Anatomy and Embryology Departments. The current protocol was revised and approved by the Institutional Animal Care and Use Committee (CU-IACUC), (approval No. CU/III/F/23/18). All procedures and animal experiments were carried out in accordance with the international Helsinki guidelines.

### Animals

Twenty four female adult albino rats were included in this study, inbred strain (Cux1: HEL1) and of matched age (6 months – 1 year) and weight (200-250 g). All animal experiments were performed according to the Guide for the Care and Use of Laboratory Animals published by the US National Institutes of Health (NIH publication No.85-23, revised 1996), and according to the standard guidelines of the Institutional Animal Care and Use Committee and after Institutional Review Board approval. Animals were maintained in an air-conditioned animal house with specific pathogen free conditions. Animals had free access to standard laboratory food and water *ad libitum*.

### Experimental design

After acclimatization, the animals were divided into 3 groups (8 rats/group). Group I (control) served as a negative control group (normal healthy rats). The remaining sixteen rats were injected with diethylnitrosamine (DEN) and carbon tetrachloride (CCl$_4$) for induction of HCC (RAGHUNANDHAKUMAR *et al.* 2013). Then, they were subdivided into 2 groups: Group II (HCC): experimental HCC group (pathological control) and Group III (HCC-Thymoquinone): HCC rats received a single intraperitoneal injection of thymoquinone (TQ) (20 mg/kg body weight) (KE *et al.* 2015) after induction of HCC. The rats were euthanized by cervical decapitation 48 hours after giving TQ.

### Induction of hepatocellular carcinoma

Hepatocarcinogenesis was induced chemically by injecting a single intra-peritoneal dose of diethylnitrosamine at a dose of 200 mg/kg body weight, followed by weekly single subcutaneous injections of carbon tetrachloride (CCl$_4$) at a dose of 3 ml/kg body weight for 6 weeks (RAGHUNANDHAKUMAR *et al.* 2013) (Fig. 1).

### Reagents:

Diethylnitrosamine (DEN): purchased from Sigma-Aldrich Egypt, number C1900 in a solution form and was given diluted with castor oil at a ratio 1:1.

Carbon tetrachloride (CCl$_4$): purchased in a solution from Sigma-Aldrich Egypt, number C1900.

Thymoquinone (TQ) (2-isopropyl-5-methyl-1,4-benzoquinone): was obtained from (Sigma-Aldrich, Tokyo, Japan) and was prepared as a 100 mM solution and stored at -30 °C until use. Olive oil (Ajinomoto, Japan) was used for dissolving the TQ. The TQ solution was prepared by dissolving it in 0.5% dimethyl sulphoxide (DMSO) followed by the addition of olive oil as previously described (ABUKHADER 2012; EL-SAYED *et al.* 2019).

At the planned time, blood was collected from each rat, for assessment of serum alanine transaminase (ALT) and aspartate transaminase (AST), and alpha fetoprotein (AFP).

The animals were then euthanized and their abdominal cavities were opened and liver tissues excised and divided into two parts. The first part was used for assessment of superoxide dismutase (SOD) and malondialdehyde (MDA), caspase-3, nuclear factor kappa-light-chain-enhancer of activated B-cell (NFκB), tumor necrosis factor-α (TNF-α), interleukin-10 (IL-10) level, gene expression of CHOP-1, Bcl-2-associated X protein (Bax) and B-cell lymphoma 2 (Bcl-2), and JNK and p38 MAPK.

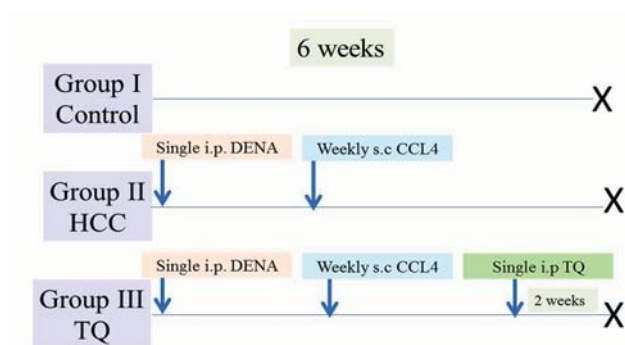The second part was fixed overnight in 40 g/l paraformaldehyde in PBS at 4°C for a histopathological

Fig. 1. Schematic representation of the experimental protocol.

examination by hematoxylin and eosin (HE) stained sections.

### Estimation of serum ALT and AST levels

Using a spectrophotometer, ALT and AST activity values were detected from the calibration curve and were expressed in U/l.

### Estimation of AFP using ELISA (Uscn, Life science Inc, UK)

A microtiter plate coated with an antibody specific to AFP was used. Then according to manufacturer protocol, the substrate reaction was spectrophotometrically measured.

### Estimation of SOD and MDA in rat liver tissue using colorimetry

After tissue homogenization, the samples were centrifuged; the supernatant was removed for assay and stored on ice. SOD Activity (U/g tissue) was estimated according to manufacturer instructions and the estimated values of MDA are expressed in mmol/mg and compared to the reference standard according to manufacturer protocol.

### Estimation of caspase-3, NFκB, TNF-α and IL-10 levels in rat liver tissue using ELISA (eBioscience, San Diego, CA, USA)

The provided microtiter plate was pre-coated with an antibody specific to caspase-3, NFκB, TNF-α, and IL-10. Standards or samples were then added. Streptavidin conjugated to Horseradish Peroxidase (HRP) was added to each microplate well and incubated. After TMB substrate solution was added, only those wells that contained (caspase-3, NFκB, TNF-α, and IL-10) biotin-conjugated antibody, and enzyme-conjugated avidin would exhibit a change in color. The enzyme-substrate reaction was terminated by the addition of an acid solution and the color change was measured using spectrophotometry at a wavelength of

450 nm. The concentration of (Caspase-3, NFκB, TNF-α, and IL-10) in the samples was then determined by comparing the O.D. of the samples to the standard curve according to manufacturer's instruction.

### qRT-PCR gene expression of CHOP, Bax, and Bcl-2 in rat liver tissues

After homogenization, total RNA was extracted from liver. The bound total RNA was further purified by simple washing steps. Finally, the total RNA was eluted from the membrane by the addition of Nuclease-Free Water. The yield of total RNA obtained was determined spectrophotometrically at 260 nm. Total RNA (0.5-2 μg) was used for cDNA conversion using a high capacity cDNA reverse transcription kit (#K1621, Fermentas, USA). Real-time qPCR amplification and analysis were performed using an Applied Biosystem with software version 3.1 (StepOne™, USA) as previously described (AZIZ et al. 2014). After the RT-PCR run, the data were expressed in Cycle threshold (Ct). The PCR data sheet includes the Ct values of the assessed genes (CHOP, Bax, and Bcl-2) and those related to the reference housekeeping gene (β-actin gene).

### Estimation of JNK and p38 MAPK using the Western Blot Technique

RIBA lysis buffer PL005 was provided by Bio BASIC INC. (Marhham Ontario L3R 8T4 Canada). The lysis buffer was added to the tissues with an additional protease inhibitor and phosphatase inhibitor buffer to maintain protein integrity and high biological activity. The supernatant was transferred to a new tube for further protein concentration determination analysis. A Bradford Protein Assay Kit (SK3041) for quantitative protein analysis was provided by BIO BASIC INC. Markham Ontario L3R 8T4 Canada. A Bradford assay was performed according to manufacture instructions. Then, the proteins were separated by polyacrylamide gel electrophoresis. The membrane was using tris-buffered saline with Tween 20 (TEST) buffer and 3% bovine serum albumin (BSA) at room temperature for 1 hr. Samples were then incubated overnight in each primary antibody solution, against the blotted target protein (anti JNK antibody and anti p38 MAPK antibody) at 4°C. Incubation was done in a HRP-conjugated secondary antibody (Goat antirabbit IgG- HRP-lmg Goat mab -Novus Biologicals) solution against the blotted target protein for 1 hour at room temperature. Chemiluminescent substrate (Clarity™ Western ECL substrate – BIO-RAD, USA cat#170-5060) was applied to the blot according to the manufacturer's recommendation. The chemiluminescent signals were captured using a CCD camera-based imager. Image analysis software was used to read the band intensity of the target proteins against the control sample after normalization by beta actin on the Chemi Doc MP imager.

Table1

Primers Sequence of studied genes CHOP, Bax, Bcl-2, and the housekeeping gene beta actin

| CHOP | Forward primer: 5'-CTGGAAGCCTGGTATGAGGAT-3'<br>Reverse primer: 5'-CAGGGTCAAGAGTAGTGAAGGT-3' |
| --- | --- |
| Bax | Forward primer: 5'-ATGGACGGGTCCGGGGAG-3'<br>Reverse primer: 5'-ATCCAGCCCAACAGCCGC-3' |
| Bcl-2 | Forward primer: 5'-AAGCCGGCGACGACTTCT-3'<br>Reverse primer: 5'-GGTGCCGGTTCAGGTACTCA-3' |
| β-actin | Forward primer: 5'-CTGAATGGCCCAGGTCTGA-3'<br>Reverse primer: 5'-CCCTGGCTGCCTCAACAC-3' |

### Histopathological examination

The liver from all groups was dissected and immediately fixed in 10% formol saline. The specimens were impregnated in paraffin. Serial sections of 5-μm thickness were cut and subjected to hematoxylin and eosin staining and histo-pathological examination.

### Statistical Analysis

Data were coded and analyzed using the Statistical Package for Social Science (SPSS) version 22 (IBM Corp., Armonk, NY, USA) and were tested for normality using the Shapiro-Wilk test and proved to not be deviated from normal distribution. Data were summarized using mean and standard deviation. Statistical significance of the differences between the mean values of the different groups was tested using Two-way analysis of variance (ANOVA) followed by Bonferroni multiple comparison post-hoc testing when comparing more than 2 groups for appraisal of statistical significance. Probability values of less than 0.05 ($p < 0.05$) were considered statistically significant.

## Results

### Improved liver function biomarkers and alpha-fetoprotein (AFP) with thymoquinone

Deterioration of liver function was observed in the HCC group and detected by a significant increase in ALT and AST levels in the HCC group compared to the normal control ($p < 0.001$). Significant increase in AFP level was observed in the HCC group compared to the normal control ($p < 0.001$). However, TQ resulted in a significant decrease in AFP level compared to the HCC group and a significant decrease in ALT and AST levels compared to the HCC group ($p < 0.001$) (Table 2).

### Interference with oxidative stress secondary to thymoquinone intake

Combined DEN and $CCL_4$ used for induction of HCC could enhance oxidative stress in the HCC group. Data showed a significant increase in MDA and a significant decrease in SOD in the HCC group compared to the normal control ($p < 0.001$), however, the intake of TQ significantly reversed these changes compared to the HCC group ($p < 0.001$) (Table 2).

### Thymoquinone enhances the host defence strategy by regulating inflammatory machinery

Data showed a significant decrease in levels of IL-10 while levels of NFκB and TNF-α were significantly increased in the HCC group compared to the normal control ($p < 0.001$). Intake of TQ resulted in a significant increase in IL-10 and a significant decrease in NFκB and TNF-α as well compared to the HCC group ($p < 0.001$) (Fig. 2).

Table 2

Serum levels of ALT, AST, AFP, MDA, and SOD among the studied groups. Values are presented as mean ±SD, (n=8). *: statistically significant compared to corresponding value in group I, and #: statistically significant compared to the corresponding value in group II

| Parameter | Group 1<br>(normal control) | Group 2 (HCC) | Group 3<br>(HCC-Thymoquinone) |
| --- | --- | --- | --- |
| ALT (U/l) | 19.75±3.5 | 79±6.58 * | 43.25±4.03 *# |
| AST (U/l) | 21.75±4.43 | 59.25±5.32 * | 36.75±3.4 *# |
| AFP (ng/ml) | 0.52±0.04 | 1.67±0.35 * | 0.82±0.14 # |
| MDA (nmol/g tissue) | 27.23±6.77 | 104.18±8.97 * | 60.23±6.25 *# |
| SOD (U/g tissue) | 4.08±0.64 | 1.45±0.42 * | 2.69±0.42 *# |

Bonferroni multiple comparisons, ANOVA, two sided p value <0.05.

**Enhanced apoptotic process in the livers of HCC rats after treatment with thymoquinone**

The key apoptotic executor, caspase-3 showed a significant increase in the HCC-thymoquinone group compared to the HCC group (p <0.001). A significant increase in Bcl-2 gene expression was also observed in the HCC group compared to the normal control (p <0.001). Whereas, levels of Bax gene expression were significantly increased in the TQ-treated groups compared to both the control and HCC groups (p <0.001) (Table 3). The data also demonstrated a significant decrease in CHOP gene expression in the HCC and HCC+TQ groups compared to the normal control (p <0.001 and p = 0.029, respectively). However, a significant increase in CHOP gene expression was observed in the TQ-treated group compared to HCC group (p <0.001) (Table 3).

**Thymoquinone upgrades the expression of p38 MAPK and JNK in liver tissues of induced HCC**

The band intensity of estimated p38 MAPK protein showed a significant increase in the HCC group and TQ-treated group compared to the normal control (p <0.001). Also, the result showed a significant increase in JNK protein expression in the TQ-treated groups compared to the control and HCC group (p <0.001) (Fig. 2).

**Thymoquinone improves the hepatic histo-patholoical changes of experimentally-induced HCC**

Combined DEN and CCL$_4$ induced pleopathological architectural and nuclear changes including nuclear atypia, pleomorphism, hyperchromatosis, and scattered mitotic figures. Thymoquinone treatment ameliorated those deleterious effects where the hepatic tissue displayed improved structure with only minimal desmoplasia and localized clear cell changes (Fig. 3).

## Discussion

Thymoquinone (TQ) is the main constituent in *Nigella sativa*; it could exert multiple anticancer effects (WOO *et al.* 2012). The anti-cancer effect of TQ is mediated through induction of apoptosis and cell cycle arrest (MAJDALAWIEH & FAYYAD 2016). In agreement with our results, TQ can ameliorate CCl$_4$-induced hepatotoxicity through suppression of lipid peroxidation, ALT and AST cleavage, and induction of caspases (RAHMANI *et al.* 2019). TQ treatment has also been reported to up-regulate JNK phosphorylation in human colon cancer cells (EL-NAJJAR *et al.* 2010) which is also concordant with our results.

Decreased expression of caspase-3 also correlates with a poor prognosis of HCC, which emphasizes the role of caspase-3 in the pathogenesis of the disease. The deficiency of caspase-3 may enhance p38 activa-
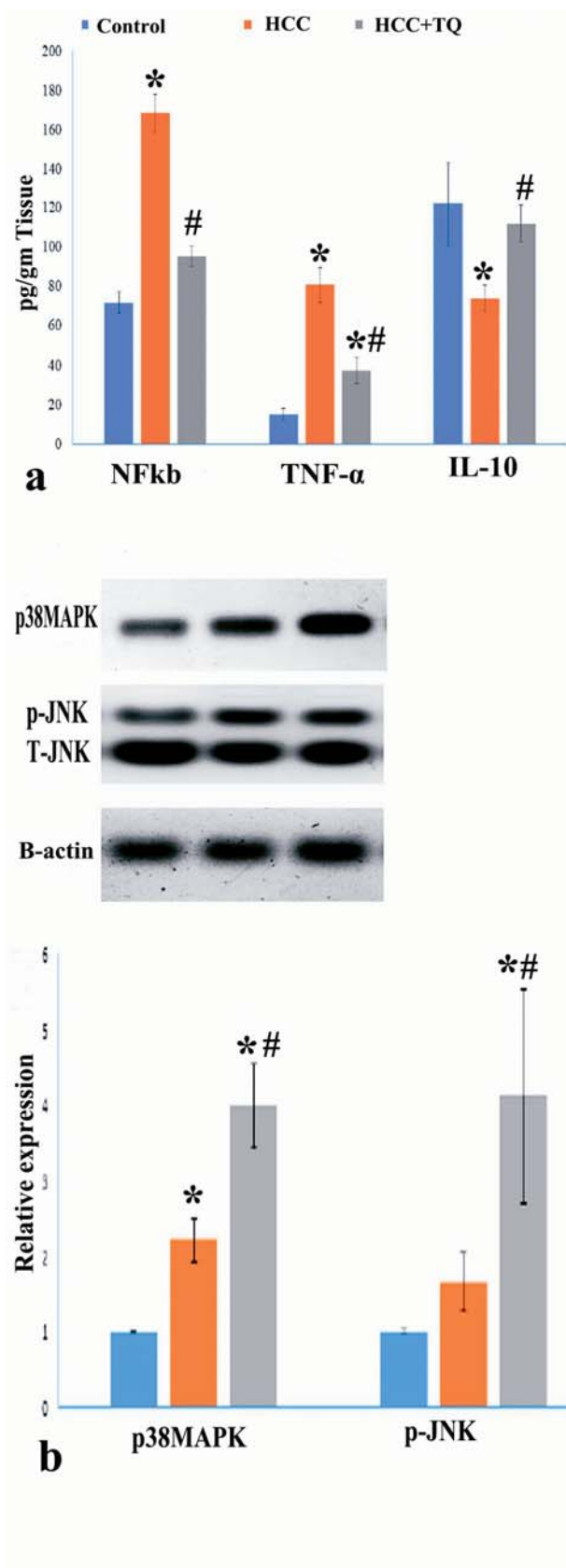


Fig. 2. (a) Anti-inflammatory effects of the natural compound, thymoquinone. (b) The expression bands and quantitative measurements of the relative gene expression of p38 MAPK and JNK (total and phosphorylated) (fold change relative to the control house keeping gene β-actin) in liver tissues. Data are expressed as mean ± SD, (n=8). P value <0.05 was significant, (*) denotes significant difference versus the normal control group, (#) denotes significant difference versus the HCC group.

Table 3

Levels of caspase-3 and the relative gene expression of Bax, Bcl-2, and CHOP-1 in all studied groups. Values presented as mean ±SD (n=8) *: statistically significant compared to corresponding value in group I and #: statistically significant compared to corresponding value in group II

| Parameter | Group 1 (normal control) | Group 2 (HCC) | Group 3 (HCC-Thymoquinone) |
|---|---|---|---|
| Caspase-3 (ng/g tissue) | 1.86±0.43 | 0.95±0.11 * | 2.83±0.22 *# |
| Bax (relative expression) | 1.01±0.02 | 0.17±0.05 | 6.2±0.92 *# |
| Bcl-2 (relative expression) | 1.01±0.01 | 4.4±0.42 * | 2.46±0.47 *# |
| CHOP-1 (relative expression) | 1.02±0.04 | 0.24±0.12 * | 0.72±0.07 *# |

Bonferroni multiple comparisons, ANOVA, two sided p value <0.05

tion in the liver tissues of mice treated with DEN by increasing the expression of TNFα (SHANG *et al.* 2018). In this regard, current results reported a significant decrease in caspase-3, and an increase in TNFα levels as well as p38 MAPK in the HCC group compared to the control group.

Deregulated MAPK signalling pathways are often implicated in various types of human tumors, as HCC (KIM *et al.* 2017), p38 MAPK negatively regulates cell cycle progression and oncogene-induced premature cell senescence thus; it acts as a tumor suppressor factor (BULAVIN & FORNACE 2004). ROS could augment and activate p38 MAPK (LIU & CHANG 2009). Moreover, TQ was found to increase p38 protein expression in liver tissues, and suppress the anti-apoptotic/pro-survival Bcl-2 gene expression as well. In this context, Torres and colleagues (TORRES *et al.* 2010) related the enhanced apoptosis in pancreatic cancer cells by TQ to its promotion of p38 MAPK and JNK signalling pathways.

JNK deficiency in liver tissues could increase hepatocyte death leading consequently to increased compensatory proliferation and HCC development (DAS *et al.* 2011). Notably, in CPT-11-R LoVo colon cancer cells, thymoquinone intake could activate JNK and p38 thereby inducing apoptosis before autophagy-mediated cell death (CHEN *et al.* 2015).

Excessive endoplasmic (ER) reticulum stress increases the C/EBP homologous protein (CHOP) marker, which is a major pro-apoptotic factor (RON & WALTER 2007). ER stress has crucial roles in mitochondrial dysfunction by augmenting CHOP expression. Incubating bladder cancer cells with TQ has also been reported to induce cytotoxicity and apoptosis, mainly through overexpression of CHOP, increasing Bax/Bcl-2 ratio and augmenting caspases (ZHANG *et al.* 2018).

Following exposure to cytotoxic agents, Bax undergoes oligmerization in the mitochondria and endoplasmic reticulum membranes, allowing for the permeabilization of these membranes, and then releases activators of the final effectors of apoptosis such as cytochrome c and SMAC/Diabalo (SHARPE *et al.* 2004; ANNIS *et al.* 2005). Thus, preventing Bax oligomerization abrogates apoptosis. However, decreased Bcl-2 could allow Bax oligomerization to induce apoptosis (DLUGOSZ *et al.* 2006). Previous studies demonstrated that CHOP promotes apoptosis by decreasing Bcl-2 expression (LIU & CHANG 2009). Our results also document enhanced CHOP expression and decreased Bcl-2. Thus, down-regulating the key factor of cell life and death is a promising target in cancer therapy.

One of the therapeutic potentials of thymoquinone is its immune-regulatory effect against HCC induced by DEN (BIMONTE *et al.* 2019). In hepatocytes, NF-κB has a contradictory effect being pro-inflammatory and anti-apoptotic, which may exert a negative impact on hepatocytes. In addition, nuclear translocation of NF-κB inhibits JNK activation (LUEDDE & SCHWABE 2011). TQ is able to suppress TNF-α-induced NF-kappa B activation (BIMONTE *et al.* 2019). Activation of NF-κB components is involved in hepatic injury, fibrosis, and subsequent carcinogenesis (LUEDDE & SCHWABE 2011). Even more, JNK activation could promote regression of the NF-κB-induced antiapoptotic factors, thus data obtained indicate that TQ may enhance cancer cell apoptosis which could decrease tumor resistance to chemotherapy and radiotherapy. Taken together, our findings suggest that TQ could be considered as a potential drug for targeting hepatocarcinogenesis via activating JNK, p38 MAPK, and enhancing production of pro-apoptotic factors including the final effector of apoptosis, caspase-3.
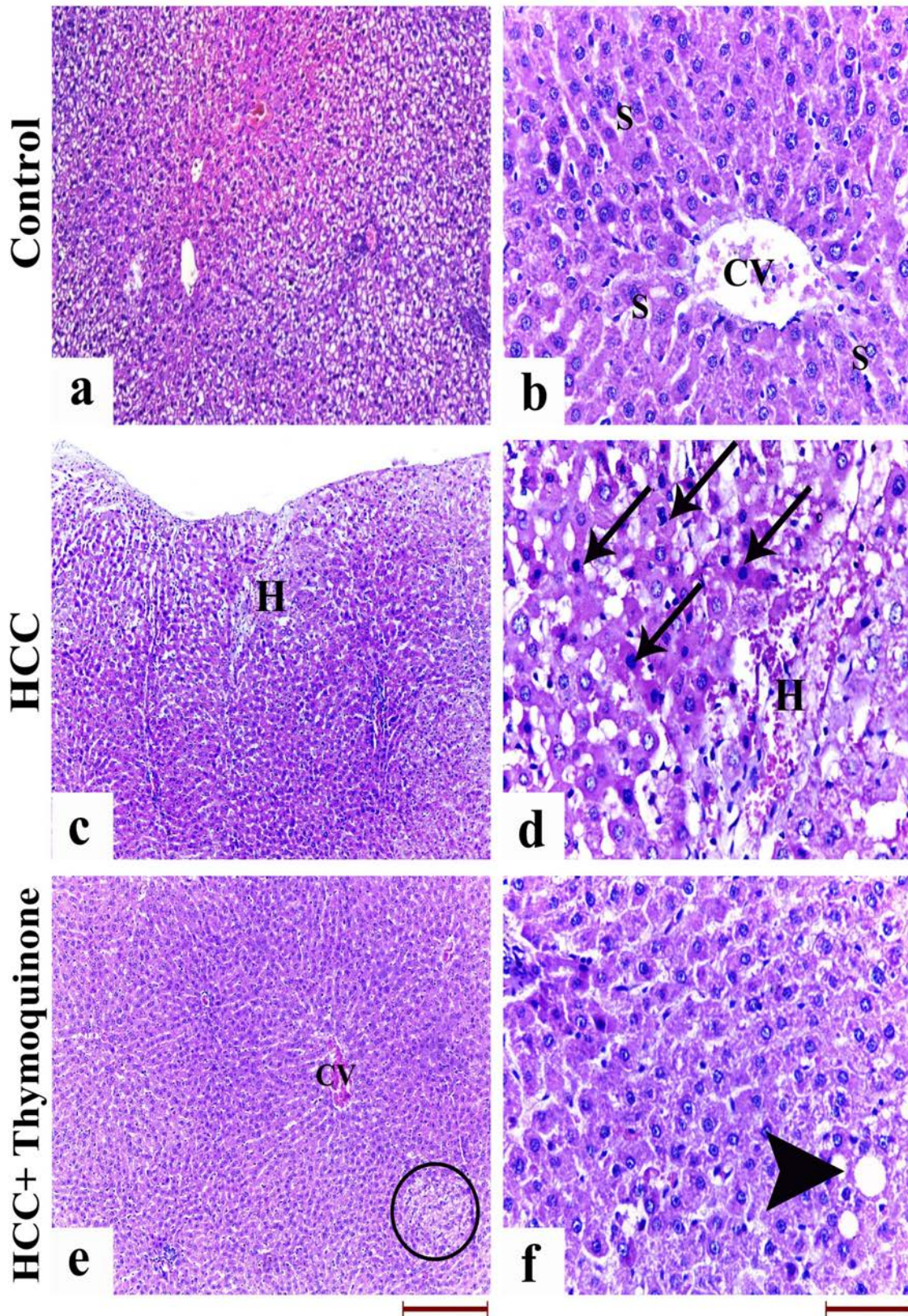
## Acknowledgements

Fig. 3. H&E-stained sections (a) Control group showing classical hepatic architecture, (b) Higher magnification of control group shows healthy hepatocytes radiating from the central vein (CV) and separated by endothelial-lined blood sinusoids (S), (c) The HCC group showing sheet arrangement of neoplastic highly proliferating hepatocytes. Areas of subcapsular hemorrhagic necrosis (H) are also noticed. (d) Higher magnification of the HCC group displays neoplastic hepatocytes with nuclear atypia, pleomorphism and hyperchromasia (arrows). (e) The HCC-thymoquinone-treated group revealing improved hepatic structure apart from localized areas of clear cell change (pseudoacinar formation) (circle) and congestion of the central vein (CV), (f) Higher magnification of the HCC-thymoquinone-treated group revealing hepatocytes with mild desmoplasia and minimal ballooning degeneration (arrow head) (a,c,e scale bar 200 μm; b,d,f scale bar 50 μm).

## Author Contributions

Research concept and design: R.E.H., G.M.A., S.A.A.E-A., H.M.; Collection and/or assembly of data: E.G.A., M.M.K.; Data analysis and interpretation: L.A.R.; Writing the article: B.E.A., A.S.E.; Critical revision of the article: B.E.A., A.S.E.; Final approval of article: B.E.A.

## Conflict of Interest

The authors declare no conflict of interest.

## References

ABUKHADER M. M. 2012. The effect of route of administration in thymoquinone toxicity in male and female rats. Indian J. Pharm. Sci. **74**: 195. Https://doi.org/10.4103/0250-474X.106060

ANNIS M.G., SOUCIE E.L., DLUGOSZ P.J., CRUZ-AGUADO J.A., PENN L.Z., LEBER B., ANDREWS D.W. 2005. Bax forms multispanning momomers that oligomerize to permeabilize membranes during apoptosis. EMBO. J. **24**: 2096-2103. https://doi.org/10.1038/sj.emboj.7600675

AZIZ M.T.A., WASSEF M.A.A., AHMED H.H., RASHED L., MAHFOUZ S., ALY M.I., HUSSEIN R.E., ABDELAZIZ M. 2014. The role of bone marrow derived-mesenchymal stem cells in attenuation of kidney function in rats with diabetic nephropathy. Diabetol. Metab. Syndr. **6**: 34. https://doi.org/10.1186/1758-5996-6-34

BHAT M., SONENBERG N., GORES G.J. 2013. The mTOR pathway in hepatic malignancies. Hepatology **58**: 810-818. Https://doi.org/10.1002/hep.26323

BIMONTE S., ALBINO V., BARBIERI A., TAMMA M.L., NASTO A., PALAIA R., MOLINO C., BIANCO P., VITALE A., SCHIANO R., GIUDICE A. 2019. Dissecting the roles of thymoquinone on the prevention and the treatment of hepatocellular carcinoma: an overview on the current state of knowledge. Infect. Agent. Cancer **14**: 10. https://doi.org/10.1186/s13027-019-0226-9

BULAVIN D.V., FORNACE A.J. 2004. p38 MAP kinase's emerging role as a tumor suppressor. Adv. Cancer. Res. **92**: 95-118. https://doi.org/10.1016/S0065-230X(04)92005-2

CHANG Y., LIN J., TSUNG A. 2012. Manipulation of autophagy by MIR375 generates antitumor effects in liver cancer. Autophagy **8**: 1833-1834. https://doi.org/10.4161/auto.21796

CHEN M.C., LEE N.H., HSU H.H., HO T.J., TU C.C., HSIEH D.J.Y., LIN Y.M., CHEN L.M., KUO W.W., HUANG C.Y. 2015. Thymoquinone induces caspase-independent, autophagic cell death in CPT-11-resistant lovo colon cancer via mitochondrial dysfunction and activation of JNK and p38. J. Agric. Food. Chem. **63**: 1540-6. https://doi.org/10.1021/jf5054063

CHIBA T., SUZUKI E., YUKI K., ZEN Y., OSHIMA M., MIYAGI S., SARAYA A., KOIDE S., MOTOYAMA T., OGASAWARA S., OOKA Y. 2014. Disulfiram eradicates tumor-initiating hepatocellular carcinoma cells in ROS-p38 MAPK pathway-dependent and -independent manners. PLoS One. **9**: e84807. https://doi.org/10.1371/journal.pone.0084807

DAS M., GARLICK D.S., GREINER D.L., DAVIS R.J. 2011. The role of JNK in the development of hepatocellular carcinoma. Genes. Dev. **25**: 634-45. Https://doi.org/10.1101/gad.1989311

DLUGOSZ P.J., BILLEN L.P., ANNIS M.G., ZHU W., ZHANG Z., LIN J., LEBER B., ANDREWS D.W. 2006. Bcl-2 changes conformation to inhibit Bax oligomerization. EMBO. J. **25**: 2287-96. https://doi.org/10.1038/sj.emboj.7601126

EL-NAJJAR N., CHATILA M., MOUKADEM H., VUORELA H., OCKER M., GANDESIRI M., SCHNEIDER-STOCK R., GALI-MUHTASIB H. 2010. Reactive oxygen species mediate thymoquinone-induced apoptosis and activate ERK and JNK signaling. Apoptosis **15**: 183-95. https://doi.org/10.1007/s10495-009-0421-z

EL-SAYED S.A.E.S., RIZK M.A., YOKOYAMA N., IGARASHI I. 2019. Evaluation of the *in vitro* and *in vivo* inhibitory effect of thymoquinone on piroplasm parasites. Parasite Vector **12**: 37. https://doi.org/10.1186/s13071-019-3296-z

HARON A.S., SYED ALWI S.S., SAIFUL YAZAN L., ABD RAZAK R., ONG Y.S., ZAKARIAL ANSAR F.H., ROSHINI ALEXANDER H. 2018. Cytotoxic Effect of Thymoquinone-Loaded Nanostructured Lipid Carrier (TQ-NLC) on Liver Cancer Cell Integrated with Hepatitis B Genome, Hep3B. Evid. Based. Complement. Alternat. Med. 1549805 https://doi.org/10.1155/2018/1549805

HU H., TIAN M., DING C., YU S. 2019. The C/EBP Homologous Protein (CHOP) Transcription Factor Functions in Endoplasmic Reticulum Stress-Induced Apoptosis and Microbial Infection. Front. Immunol. **9**: 3083. https://doi.org/10.3389/fimmu.2018.03083

IYODA K., SASAKI Y., HORIMOTO M., TOYAMA T., YAKUSHIJIN T., SAKAKIBARA M., TAKEHARA T., FUJIMOTO J., HORI M., WANDS J.R., HAYASHI N. 2003. Involvement of the p38 mitogen-activated protein kinase cascade in hepatocellular carcinoma. Cancer **97**: 3017-3026. https://doi.org/10.1002/cncr.11425

KE X., ZHAO Y., LU X., WANG Z., LIU Y., REN M., LU G., ZHANG D., SUN Z., XU Z., SONG J.H. 2015. TQ inhibits hepatocellular carcinoma growth *in vitro* and *in vivo* via repression of Notch signaling. Oncotarget **6**: 32610. https://doi.org/10.18632/oncotarget.5362

KIM S.Y., KYAW Y.Y., CHEONG J. 2017. Functional interaction of endoplasmic reticulum stress and hepatitis B virus in the pathogenesis of liver diseases. World. J. Gastroenterol. **23**: 7657-7665. Https://doi.org/10.3748/wjg.v23.i43.7657

LUEDDE T., SCHWABE R.F. 2011. NF-κB in the liver – linking injury, fibrosis and hepatocellular carcinoma. Nat. Rev. Gastroenterol. Hepatol. **8**: 108. https://doi.org/10.1038/nrgastro.2010.213

LIU W.H., CHANG L.S. 2009. Reactive oxygen species and p38 mitogen-activated protein kinase induce apoptotic death of U937 cells in response to *Naja nigricollis* toxin-gamma. J. Cell. Mol. Med. **13**: 1695-705. https://doi.org/10.1111/j.1582-4934.2008.00473.x

MAJDALAWIEH A.F.. FAYYAD M.W. 2016. Recent advances on the anti-cancer properties of *Nigella sativa*, a widely used food additive. J. Ayurveda. Integr. Med. **7**: 173-80. https://doi.org/10.1016/j.jaim.2016.07.004

OZAKYOL A. 2017. Global epidemiology of hepatocellular carcinoma (HCC epidemiology). J. Gastrointest. Cancer **48**: 238-240. https://doi.org/10.1007/s12029-017-9959-0

PARK E.J., CHAUHAN A.K., MIN K.J., PARK D.C., KWON T.K. 2016. Thymoquinone induces apoptosis through downregulation of c-FLIP and Bcl-2 in renal carcinoma Caki cells. Oncol. Rep. **36**: 2261-7. https://doi.org/10.3892/or.2016.5019

PARK G. B., CHOI Y., KIM Y. S., LEE H. K., KIM D., HUR D. Y. 2014. ROS-mediated JNK/p38-MAPK activation regulates Bax translocation in Sorafenib-induced apoptosis of EBV-transformed B cells. Int. J. Oncol. **44**: 977-85. https://doi.org/10.3892/ijo.2014.2252

RAGHUNANDHAKUMAR S., PARAMASIVAM A., SENTHILRAJA S., NAVEENKUMAR C., ASOKKUMAR S., BINUCLARA J., JAGAN S., ANANDAKUMAR P., DEVAKI T. 2013. Thymoquinone inhibits cell proliferation through regulation of G1/S phase cell cycle transition in N-nitrosodiethylamine-induced experimental rat hepatocellular carcinoma. Toxicol. Lett. **223**: 60-72. https://doi.org/10.1016/j.toxlet.2013.08.018

RAHMANI A.H., ALMATROUDI A., BABIKER A.Y., KHAN A.A., ALSAHLI M.A. 2019. Thymoquinone, an Active Constituent of Black Seed Attenuates CCl4 Induced Liver Injury in Mice via Modulation of Antioxidant Enzymes, PTEN, P53 and VEGF Protein. Open Access Maced. J. Med. Sci. **7**: 311-317. https://doi.org/0.3889/oamjms.2019.050

RON D., WALTER P. 2007. Signal integration in the endoplasmic reticulum unfolded protein response. Nat. Rev. Mol. Cell Biol. **8**: 519-29. https://doi.org/10.1038/nrm2199

SHANG N., BANK T., DING X., BRESLIN P., LI J., SHI B., QIU W. 2018. Caspase-3 suppresses diethylnitrosamine-induced hepatocyte death, compensatory proliferation and hepatocarcino-

genesis through inhibiting p38 activation. Cell. Death. Dis. **9**: 558. https://doi.org/10.1038/s41419-018-0617-7

SHARPE J.C., ARNOULT D., YOULE R.J. 2004. Control of mitochondrial permeability by Bcl-2 family members. Biochim. Biophys. Acta **1644**: 107-113.
https://doi.org/10.1016/j.bbamcr.2003.10.016

TORRES M.P., PONNUSAMY M.P., CHAKRABORTY S., SMITH L.M., DAS S., ARAFAT H.A., BATRA S.K. 2010. Effects of thymoquinone in the expression of mucin 4 in pancreatic cancer cells: implications for the development of novel cancer therapies. Mol. Cancer. Ther. **9**: 1419-31.
https://doi.org/10.1158/1535-7163.MCT-10-0075

WANG W.A., GROENENDYK J., MICHALAK M. 2014. Endoplasmic reticulum stress associated responses in cancer. Biochim. Biophys. Acta **1843**: 2143-2149.
https://doi.org/10.1016/j.bbamcr.2014.01.012

WOO C.C., KUMAR A.P., SETHI G., TAN K.H.B. 2012.Thymoquinone: potential cure for inflammatory disorders and cancer. Biochem. Pharmacol. **83**: 443-51.
https://doi.org/10.1016/j.bcp.2011.09.029

ZHANG M., DU H., HUANG Z., ZHANG P., YUE Y., WANG W., LIU W., ZENG J., MA J., CHEN G. WANG X. 2018. Thymoquinone induces apoptosis in bladder cancer cell via endoplasmic reticulum stress-dependent mitochondrial pathway. Chem. Biol. Interact. **292**: 65-75. https://doi.org/10.1016/j.cbi.2018.06.013